

Contribution from the Laboratoire de Synthèse et d'Electrosynthèse Organométallique, Associé au CNRS (UA 33), Université de Bourgogne, Faculté des Sciences "Gabriel", 6 Boulevard Gabriel, 21100 Dijon, France, and Department of Chemistry, University of Houston, Houston, Texas 77204-5641

Synthesis and Characterization of Tin(IV) Porphyrins with S²⁻ and Se²⁻ Axial Ligands

R. Guillard,*^{1a} C. Ratti,^{1a,b} J.-M. Barbe,^{1a} D. Dubois,^{1b} and K. M. Kadish*^{1b}

Received June 8, 1990

The reaction of Cp₂TiS₃ or Cp₂TiSe₃ with divalent tin porphyrins of the form (P)Sn leads to the formation of (P)SnS or (P)SnSe, where P is the dianion of tetraphenylporphyrin (TPP), tetra-*m*-tolylporphyrin (TmTP), tetra-*p*-tolylporphyrin (TpTP), tetramesitylporphyrin (TMP), or octaethylporphyrin (OEP). These pentacoordinated compounds provide the first examples for the binding of chalcogen axial ligands and an oxo type ligation in main-group metalloporphyrins. Each synthesized complex was characterized by mass spectrometry, IR, UV-visible, and ¹H NMR spectroscopies as well as by electrochemistry.

Introduction

The chemistry and physicochemical properties of group 14 metalloporphyrins have been extensively studied in aqueous and nonaqueous media. Many of the porphyrins have been examined with respect to their photochemistry,²⁻⁹ while others have been studied with respect to their activity as inhibitors of heme oxygenase.¹⁰

Most group 14 metalloporphyrins are stable in the +4 oxidation state and exhibit a trans hexacoordination scheme with either ionic¹¹⁻¹⁸ or σ -bonded axial ligands.^{12,18-23} An oxo ligation is also possible with many metalloporphyrins containing +4 central metals, but this type of bonding scheme has never been observed for main-group metalloporphyrins. On the other hand, an oxo type ligation of chalcogen ligands with V(IV) porphyrins has been reported by using V(II) complexes as precursors,²⁴ and our recent

Table I. Yields and IR Data for (P)SnS and (P)SnSe^a

porphyrin P	axial ligand X	recryst solvent ^b	% yield	wavenumber, cm ⁻¹ Sn=X
TPP	S ²⁻	A	39	437
TmTP		B	60	433
TpTP		A/B (2/1)	58	432
TMP		A/B (2/1)	40	434
OEP		c	91	426
TPP	Se ²⁻	A	47	300
TmTP		B	57	298
TpTP		B	67	298
TMP		A/B (2/1)	89	297
OEP		c	89	292

^aMicroanalyses were obtained by "Service de Microanalyses du CNRS" and gave the following satisfactory data: C, $\pm 0.50\%$; H, $\pm 0.1\%$; N, $\pm 0.3\%$; S, $\pm 0.2\%$; Se, $\pm 0.4\%$. ^bSolvents: A, toluene; B, heptane. ^cSee Experimental Section.

- (1) (a) Université de Bourgogne. (b) University of Houston.
- (2) Whitten, D. G.; Yau, J. C.; Carroll, F. A. *J. Am. Chem. Soc.* **1971**, *93*, 2291.
- (3) Whitten, D. G.; Yau, J. C. *Tetrahedron Lett.* **1969**, *36*, 3077.
- (4) Szulbinski, W.; Zak, J.; Strojek, J. W. *J. Electroanal. Chem. Interfacial Electrochem.* **1987**, *226*, 157.
- (5) Szulbinski, W.; Strojek, J. W. *Inorg. Chim. Acta* **1986**, *118*, 91.
- (6) Inoue, H.; Chandrasekaran, K.; Whitten, D. G. *J. Photochem.* **1985**, *30*, 269.
- (7) Chandrasekaran, K.; Giannotti, C.; Monserrat, K.; Otruba, J. P.; Whitten, D. G. *J. Am. Chem. Soc.* **1982**, *104*, 6200.
- (8) Fuhrhop, J.-H.; Kruger, W.; David, H. H. *Liebigs Ann. Chem.* **1983**, *204*.
- (9) Harel, Y.; Manassen, J. *J. Am. Chem. Soc.* **1977**, *99*, 5817.
- (10) (a) Delaney, J. K.; Mauzerall, L.; Drummond, G. S.; Kappas, A. *Pediatrics* **1988**, *81*, 498 and references therein. (b) Stout, D. L.; Becker, F. F. *Drug Metab. Dispos.* **1988**, *16*, 23 (see also references therein). (c) Kappas, A.; Drummond, G. S.; Manola, T.; Petmezaki, S.; Valaes, T. *Pediatrics* **1988**, *81*, 485 and references therein.
- (11) Buchler, J. W.; Puppe, L.; Rohbock, K.; Schneehage, H. H. *Chem. Ber.* **1973**, *106*, 2710.
- (12) Kadish, K. M.; Xu, Q. Y.; Barbe, J.-M.; Anderson, J. E.; Wang, E.; Guillard, R. *J. Am. Chem. Soc.* **1987**, *109*, 7705.
- (13) Kadish, K. M.; Xu, Q. Y.; Maya, G. B.; Barbe, J.-M.; Guillard, R. *J. Chem. Soc., Dalton Trans.* **1989**, 1531.
- (14) Gouterman, M.; Schwarz, T. P.; Smith, P. D.; Dolphin, D. J. *Chem. Phys.* **1973**, *59*, 676.
- (15) Treibs, A. *Liebigs Ann. Chem.* **1969**, *728*, 115.
- (16) Guillard, R.; Barbe, J.-M.; Boukhris, A.; Lecomte, C.; Anderson, J. E.; Xu, Q. Y.; Kadish, K. M. *J. Chem. Soc., Dalton Trans.* **1988**, 1109.
- (17) Kadish, K. M.; Xu, Q. Y.; Barbe, J.-M.; Anderson, J. E.; Wang, E.; Guillard, R. *Inorg. Chem.* **1988**, *27*, 691.
- (18) Kadish, K. M.; Xu, Q. Y.; Barbe, J.-M.; Guillard, R. *Inorg. Chem.* **1988**, *27*, 1191.
- (19) Cloutour, C.; Lafargue, D.; Richards, J. A.; Pommier, J.-C. *J. Organomet. Chem.* **1977**, *137*, 157.
- (20) Guillard, R.; Kadish, K. M. *Chem. Rev.* **1988**, *88*, 1121.
- (21) Xu, Q. Y.; Barbe, J.-M.; Kadish, K. M. *Inorg. Chem.* **1988**, *27*, 2373.
- (22) Cloutour, C.; Lafargue, D.; Pommier, J.-C. *J. Organomet. Chem.* **1978**, *161*, 327.
- (23) Cloutour, C.; Debaig-Valade, C.; Gacherieu, C.; Pommier, J.-C. *J. Organomet. Chem.* **1984**, *269*, 239.
- (24) Poncet, J.-L.; Guillard, R.; Friand, P.; Goulon-Ginet, C.; Goulon, J. *Nouv. J. Chim.* **1984**, *8*, 583.

isolation of tin(II) porphyrins²⁵ suggested that similar types of derivatives might be synthesized for complexes with a Sn(IV) central metal. This is indeed the case, as demonstrated in the present paper.

The synthesized porphyrins are represented by (P)SnS and (P)SnSe, where P is the dianion of tetraphenylporphyrin (TPP), tetra-*m*-tolylporphyrin (TmTP), tetra-*p*-tolylporphyrin (TpTP), tetramesitylporphyrin (TMP), or octaethylporphyrin (OEP). Each metalloporphyrin was characterized by mass spectrometry, IR, UV-visible, and ¹H NMR spectroscopies as well as by electrochemistry.

Experimental Section

Chemicals. Synthesis and handling of the metalloporphyrins were carried out under an argon atmosphere. All solvents were thoroughly dried in an appropriate manner under an inert argon atmosphere using Schlenk techniques. (P)Sn were prepared according to literature procedures.²⁵ Tetrabutylammonium perchlorate (TBAP) was purchased from Eastman Kodak Co., twice recrystallized from absolute ethanol, and dried in a vacuum oven at 40 °C prior to use.

General Procedure for Preparation of (P)SnS and (P)SnSe. A 0.88-mmol sample of Cp₂TiS₃ or Cp₂TiSe₃ was added to 0.51 mmol of (P)Sn in 100 mL of toluene (or THF) while being stirred vigorously. After 15 min the solvent was removed by evaporation and the crude product chromatographed on a basic alumina-packed column that had previously been dried under vacuum for 2 h at 250 °C. The eluent was a 1:2 toluene/tetrahydrofuran mixture. The solution was evaporated and the solid recrystallized to give a final yield that ranged from 39 to 91%. The exact yield of each synthesized complex is given in Table I.

All of the compounds were examined in solution except for (OEP)SnS and (OEP)SnSe, both of which had a very low solubility in all organic solvents, thus preventing solution studies from being carried out. However, mass spectra could be obtained for these compounds by direct introduction of the solid into the mass spectrometer.

Instrumentation. Mass spectra were recorded in the electron-impact mode with a VG ZAB2-SEQ spectrometer (ionizing energy 70 eV, ion-

- (25) Barbe, J.-M.; Ratti, C.; Richard, P.; Lecomte, C.; Gérardin, R.; Guillard, R. *Inorg. Chem.* **1990**, *29*, 4126.

Table II. UV-Visible Data for (P)SnS and (P)SnSe in Toluene

porphyrin P	axial ligand	λ_{\max} , nm ($10^{-3}\epsilon$)					
		Soret region		visible region			
TPP	S ²⁻	342 (24.2)	436 (311.6)	529 (3.0)	567 (12.9)	608 (7.5)	
TmTP		341 (25.8)	436 (375.0)	526 (3.2)	568 (14.8)	609 (8.3)	
TpTP		342 (24.4)	437 (394.4)	524 (3.6)	569 (14.6)	611 (10.2)	
TMP		335 (27.9)	437 (365.4)	526 (7.4)	566 (19.3)	608 (10.9)	630 (6.0)
TPP	Se ²⁻	340 (30.3)	437 (334.2)	524 (2.8)	567 (11.7)	609 (6.4)	639 (1.5)
TmTP		339 (35.4)	439 (407.1)	525 (3.2)	568 (14.1)	609 (8.0)	638 (1.4)
TpTP		341 (31.5)	439 (366.4)	534 (3.2)	570 (12.4)	611 (8.8)	638 (2.2)
TMP		337 (40.3)	440 (433.9)	532 (3.4)	571 (13.3)	612 (7.4)	643 (3.9)

Table III. ¹H NMR Spectroscopic Data for (P)SnS and (P)SnSe at 294 K in C₆D₆

porphyrin P	axial ligand	pyrrole H		ortho H		meta H		para H		ortho CH ₃		meta CH ₃		para CH ₃		
		δ^a	m/i ^b	δ	m/i	δ	m/i	δ	m/i	δ	m/i	δ	m/i	δ	m/i	
TPP	S ²⁻	9.04	s/8	7.94	m/4	7.47	m/8	7.40	m/4							
TmTP		9.14	s/8	7.88	d/4	7.36	m/4 ^c	7.36	m/4 ^c			2.32	s/6			
TpTP		9.17	s/8	7.89	m/8	7.25	m/8					2.30	s/6			
TMP		9.03	s/8			7.12	s/8					1.88	s/12		2.39	s/12
TPP	Se ²⁻	9.03	s/8	7.94	m/8	7.48	m/8	7.40	m/4							
TmTP		9.13	s/8	7.94	s/4	7.34	m/4 ^c	7.34	m/4 ^c			2.32	s/6			
TpTP		9.16	s/8	7.91	m/8	7.24	m/8					2.28	s/6		2.38	s/12
TMP		9.02	s/8			7.13	s/8					1.92	s/12		2.40	s/12
											1.88	s/12				

^a δ , ppm. ^bm/i: multiplicity/intensity. s = singlet; d = doublet; t = triplet; m = multiplet. ^cOverlapped meta and para H signals.

izing current 0.2 mA, source temperature 250–500 °C). Infrared spectra were obtained on a Perkin-Elmer 580B instrument and were recorded as 1% dispersions in CsI pellets. Electronic absorption spectra were recorded on a Perkin-Elmer 559 spectrophotometer or on an IBM Model 9430 spectrophotometer. ¹H NMR spectra were recorded at 400 MHz on a Bruker WM 400 spectrometer of the Cerema "Centre de Résonance Magnétique de l'Université de Bourgogne". Spectra were taken of 0.5-mL solutions in C₆D₆ with tetramethylsilane as internal reference. Cyclic voltammograms were recorded with a three-electrode system using an IBM EC 225 voltammetric analyzer connected to a Houston Instruments 2000 X-Y recorder. The working electrode was a platinum button, and the counter electrode, a platinum wire. A home-built saturated calomel electrode (SCE) was used as the reference electrode and was separated from the bulk of the solution by a fritted-glass bridge. Bulk controlled-potential coulometry was performed in a Vacuum Atmosphere glovebox with an EG&G Model 173 potentiostat. An EG&G Model 179 digital coulometer was used to record the current-time curves and the total charge transferred during electrolysis. Thin-layer spectroelectrochemical measurements were performed with an EG&G Model 173 potentiostat coupled with a Tracor Northern 6500 rapid-scan spectrometer. The utilized optically transparent platinum thin-layer electrode (OTTLE) has been described in a previous publication.²⁶ Tetrabutylammonium perchlorate (TBAP) was used as supporting electrolyte and was 0.1 M for all electrochemical measurements.

Results and Discussion

Spectroscopic Data. Mass spectral data permit one to establish the molecular formula of each synthesized complex. The molecular peak is weak for each (P)SnS (1–10%) or (P)SnSe (3–15%) derivative, and in all cases the parent peak is the ionic [(P)Sn]⁺ species. No peaks for dimeric forms of the two complexes were observed. The relative intensity of the molecular peak is larger for the complexes with a more basic porphyrin ring in both the (P)SnS and (P)SnSe series and is highest for the TMP and OEP derivatives which appear to be the most stable. Also, the (P)SnSe complexes have stronger relative molecular peak intensities than the analogous (P)SnS derivatives, thus suggesting that metalloporphyrins in the Se²⁻ series are more stable than those in the S²⁻ series. The mass spectral data for (P)SnS and (P)SnSe contrast with data for (P)VS and (P)VSe²⁴ or (P)Ti(S₂) and (P)Ti(Se₂),²⁷ both of which show molecular peaks for the sulfur

derivatives that are larger in intensity than those of the Se complexes.

Metal-chalcogen IR stretching frequencies of the (P)SnS and (P)SnSe complexes in the solid state are listed in Table I. There is a strong metal-chalcogen stretching band between 437 and 426 cm⁻¹ for (P)SnS and between 300 and 292 cm⁻¹ for (P)SnSe. These bands are located at 432 cm⁻¹ for (TpTP)SnS and at 298 cm⁻¹ for (TpTP)SnSe. The values for (P)SnS are higher in frequency than is usually observed for Sn-SR (300–400 cm⁻¹)²⁸ or Sn-S-Sn vibrators (315–390 cm⁻¹).²⁸ Absorption bands for Sn=S and Sn=Se are located at 487 and 331 cm⁻¹, respectively,²⁸ and are close to values for (P)SnS and (P)SnSe, which indicate a double bond between the chalcogen axial ligand and the Sn(IV) atom.

UV-visible data of the investigated complexes are summarized in Table II. Each (P)SnS and (P)SnSe derivative has a strong Soret band in the range 436–440 nm and a weaker band between 335 and 342 nm. The intensity of the latter band is larger for (P)SnSe than for (P)SnS. Three Q bands are also observed between 524 and 611 nm for (P)SnS when P = TPP, TmTP, or TpTP. This contrasts with spectra of (TMP)SnS and the (P)SnSe complexes, all of which exhibit four, rather than three Q bands between 524 and 643 nm. A similar spectrum with four visible bands has also been reported for (P)Sn(SO₃CF₃)₂ in toluene.²⁹

Figure 1 illustrates the UV-visible spectrum of (TmTP)SnS and (TmTP)SnSe in toluene. Both spectra belong to the "normal porphyrin class".³⁰ The spectra are similar to each other and are also similar in shape to UV-visible spectra of (P)SnX₂ where X = Cl⁻, Br⁻, F⁻, ClO₄⁻, or OH⁻.¹³ However the Soret and visible bands of (P)SnS and (P)SnSe are red-shifted by 7–10 nm compared to bands of (P)SnX₂ with the same porphyrin ring.

¹H NMR Data. ¹H NMR spectra of (TmTP)SnS and (TmTP)SnSe are shown in Figure 2, and data for the eight complexes investigated by ¹H NMR are summarized in Table III. Each

(27) Guilard, R.; Ratti, C.; Richard, P.; Tabard, A.; Dubois, D.; Kadish, K. M. *Inorg. Chem.* **1990**, *29*, 2532.

(28) Maslowsky, E. *Vibrational Spectra of Organometallic Compounds*; J. Wiley and Sons: New York, 1977.

(29) Barbe, J.-M. Dissertation, Université de Bourgogne, 1985.

(30) Gouterman, M. In *The Porphyrins*; Dolphin, D., Ed.; Academic: New York, 1978; Vol. III, Chapter 1.

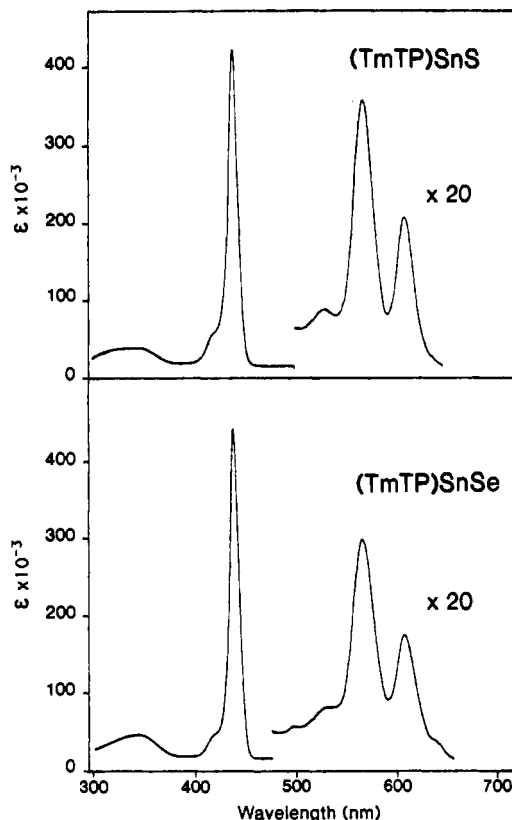


Figure 1. UV-visible spectra of (TmTP)SnS and (TmTP)SnSe in toluene.

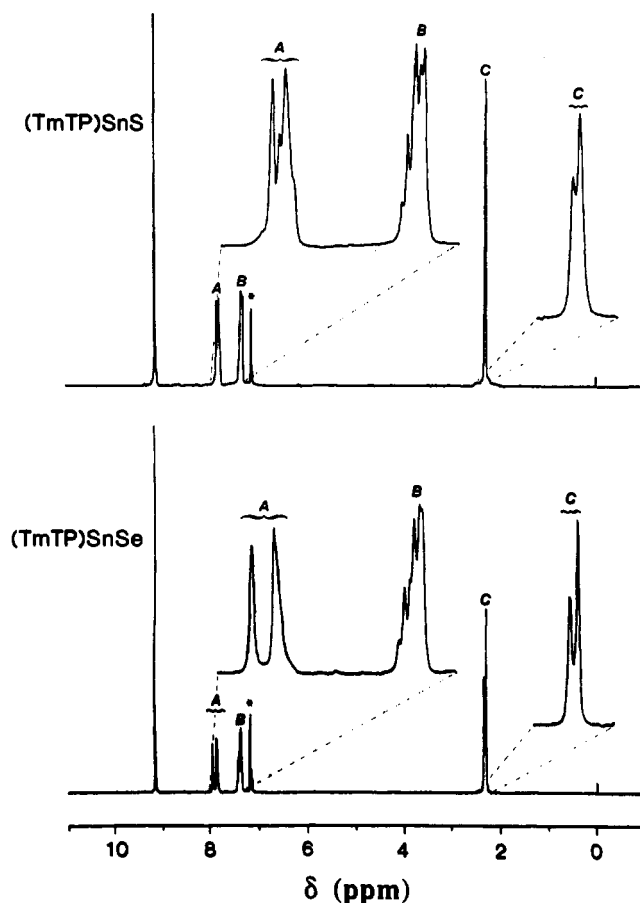


Figure 2. ¹H NMR spectra of (TmTP)SnS and (TmTP)SnSe at 294 K in C₆D₆ (asterisk = solvent).

chalcogen derivative has features typical of a diamagnetic tin(IV) porphyrin.³¹ The ortho protons (labeled as peak A in Figure 2)

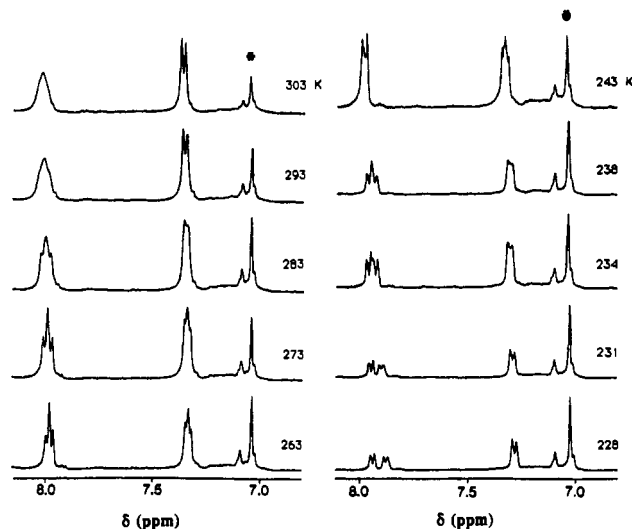


Figure 3. ¹H NMR spectra of (TpTP)SnSe in toluene between 303 and 228 K. (asterisk = solvent).

Table IV. Half-Wave Potentials (V vs SCE) for the Reduction and Oxidation of (P)SnS and (P)SnSe in CH₂Cl₂, 0.1 M TBAP

porphyrin P	axial ligand	redn			oxidn
		E _{1/2}	E _{1/2}	ΔE _{1/2}	E _p ^a
TPP	S ²⁻	-0.85	-1.24	0.39	0.85
	Se ²⁻	-0.87	-1.26	0.39	0.72
TmTP	S ²⁻	-0.90	-1.27	0.37	0.66
	Se ²⁻	-0.91	-1.29	0.38	0.63
TpTP	S ²⁻	-0.88	-1.27	0.39	0.70
	Se ²⁻	-0.91	-1.29	0.38	0.70
TMP	Se ²⁻	-0.99	-1.45	0.46	0.85

^a First scan measured at 0.1 V/s.

appear as a singlet and a multiplet. These resonances are located at 7.88 and 7.83 ppm for (TmTP)SnS and at 7.94 and 7.84 ppm for (TmTP)SnSe. This is in agreement with the nonequivalence of both sides of the macrocycle and suggests that the Sn(IV) ion is out of the macrocyclic plane. Moreover, two signals appear for the meta CH₃ protons. This is consistent with two of the four CH₃ groups being located on one side of the macrocycle with the other two being located on the opposite side. The meta and para protons (labeled as peak B in Figure 2) appear as a single overlapped broad peak at 7.36 ppm for (TmTP)SnS and 7.34 ppm (TmTP)SnSe (see Table III).

The ortho proton resonances of (TpTP)SnS and (TpTP)SnSe appear as a single broad signal. This is also the case for (TpTP)Sn²⁵ and may be explained by a free rotation of the phenyl rings, which induces an equivalence of the ortho protons.³² The ¹H NMR spectra of (P)SnS and (P)SnSe were measured over a range of temperatures, and the resulting data for one of the complexes, (TpTP)SnSe, is shown in Figure 3. As the temperature is decreased from 303 to 228 K, the single ortho proton peak at 7.91 ppm splits into two doublets, which at 228 K are located at 7.83 and 7.93 ppm. The meta protons also become nonequivalent with decrease in temperature and a double doublet is observed at 263 K.

The ortho CH₃ substituents of (TMP)SnS and (TMP)SnSe exhibit two well-separated singlets close to 1.9 ppm (see Table III). This can be explained by the slow aryl group rotation due to steric hindrance induced by the TMP ligand.³³

Electroreduction of (P)SnS and (P)SnSe. The electrochemical behavior of seven (P)SnS and (P)SnSe complexes was examined in CH₂Cl₂ containing 0.1 M TBAP as supporting electrolyte. Each

(31) Scherer, H.; Katz, J. J. In *Porphyrins and Metalloporphyrins*; Smith, K. M., Ed.; Amsterdam, 1975; p 399.

(32) Eaton, S. S.; Eaton, G. R. *J. Am. Chem. Soc.* 1977, 99, 6594.

(33) Eaton, S. S.; Eaton, G. R. *J. Am. Chem. Soc.* 1975, 97, 3660.

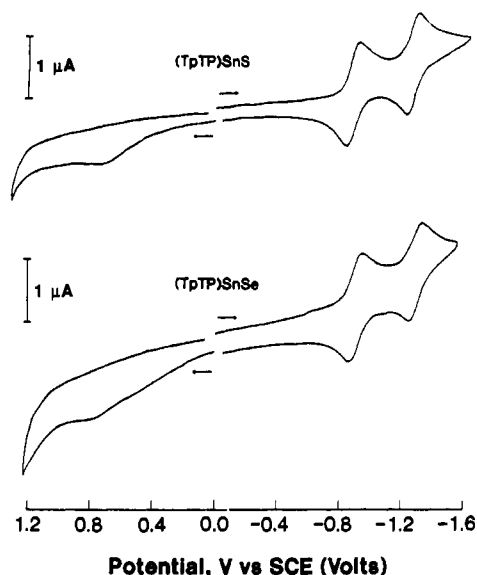


Figure 4. Cyclic voltammograms of (TpTP)SnS and (TpTP)SnSe in CH_2Cl_2 , 0.1 M TBAP. Scan rate = 0.1 V/s.

metalloporphyrin undergoes two reversible reductions up to the solvent potential limit of -2.00 V vs SCE. Values of half-wave or peak potentials as obtained by cyclic voltammetry are summarized in Table IV, while Figure 4 illustrates cyclic voltammograms for the oxidation and reduction of (TpTP)SnS and (TpTP)SnSe in CH_2Cl_2 , 0.1 M TBAP.

Conventional analysis of the cyclic voltammograms shows each reduction to involve a diffusion-controlled one-electron transfer. The selenium derivatives are more difficult to reduce by 20–30 mV as compared to the sulfur complexes with the same porphyrin ring. The $E_{1/2}$ for reduction of the four TmTP and TpTP derivatives are also close to $E_{1/2}$ values for reduction of (TmTP)-Sn(OH)₂ or (TpTP)Sn(OH)₂ in CH_2Cl_2 .³⁴ Similar potentials are recorded in THF for these latter compounds,¹³ and the reactions have been characterized as involving electron additions to the porphyrin π ring system to give π anion radicals and dianions under these solution conditions.

The formation of porphyrin π anion radicals and dianions upon reduction of (P)SnSe or (P)SnS is also suggested by the relative $E_{1/2}$ values for electroreduction of each complex. The potential difference between the two reductions of (P)SnS or (P)SnSe varies between 0.37 and 0.46 V and is within the range of the 0.42 ± 0.03 V separation generally observed for ring-centered reductions of TPP or OEP metalloporphyrins.³⁵ These separations in $E_{1/2}$ also compare well with the 0.37–0.42 V difference in $E_{1/2}$ often observed for other Sn(IV) porphyrins with ionic axial ligands.^{34,36}

The UV-visible spectra of selected complexes were monitored as a function of time during controlled-potential thin-layer reduction.³⁷ Maximum wavelengths and molar absorptivities of each neutral and singly stable reduced complex are reported in Table V, while Figure 5 illustrates time-resolved spectra recorded

(34) Half-wave potentials for the reduction of (P)Sn(OH)₂ in CH_2Cl_2 , 0.1 M TBAP as measured in our laboratory by cyclic voltammetry vs an SCE reference are as follows: (TpTP)Sn(OH)₂, $E_{1/2} = -0.98$ and -1.36 V; (TmTP)Sn(OH)₂, $E_{1/2} = -0.97$ and -1.35 V.

(35) Kadish, K. M. *Prog. Inorg. Chem.* **1986**, *34*, 435–605.

(36) Half-wave potentials for the reduction of (P)SnF₂ in CH_2Cl_2 , 0.1 M TBAP as measured in our laboratory by cyclic voltammetry vs an SCE reference are as follows: (TPP)SnF₂, $E_{1/2} = -0.87$ and -1.29 V; (TmTP)SnF₂, $E_{1/2} = -0.87$ and -1.27 V; (TpTP)SnF₂, $E_{1/2} = -0.83$ and -1.20 V.

(37) Porphyrin decomposition was encountered during spectroelectrochemical measurements of (TmTP)SnS, (TmTP)SnSe, and (TmTP)SnSe, thus preventing spectral data from being obtained for these three reduced complexes. However, cyclic voltammetric and bulk electrolysis data for these species are in good agreement with the overall behavior of the more stable TPP and TpTP derivatives and suggest that the same electrooxidation/reduction mechanism occurs for all of the investigated compounds.

Table V. Maximum Absorbance Wavelengths and Molar Absorptivities of Neutral, Reduced, and Oxidized Sn(IV) Complexes in CH_2Cl_2 , 0.1 M TBAP

porphyrin ring P	axial ligand	λ_{max} , nm ($10^{-4}\epsilon$)		
		neutral	reduced ^a	oxidized ^a
TPP	S ²⁻	432 (41.0)	427 ^b	426 (41)
		565 (2.8)	449 (12)	559 (3)
		606 (1.9)		601 (2)
TPP	Se ²⁻	434	425 ^b	421
		567	437 ^b	556
		608	450	595
TpTP	S ²⁻	433 (36.8)	428 (12)	428 (34)
		565 (2.4)	451 (11)	562 (2)
		606 (1.9)		604 (1)
TpTP	Se ²⁻	436 (35.3)	428 (8)	425 (45)
		566 (2.5)	452 (9)	557 (3)
		607 (2.1)		597 (1)
TpTP	(ClO ₄) ₂	425 (56.0)		
		557 (2.9)		
		598 (2.1)		

^a Estimated precision in ϵ values for the reduced and oxidized species is $\pm 10\%$. ^b Shoulder.

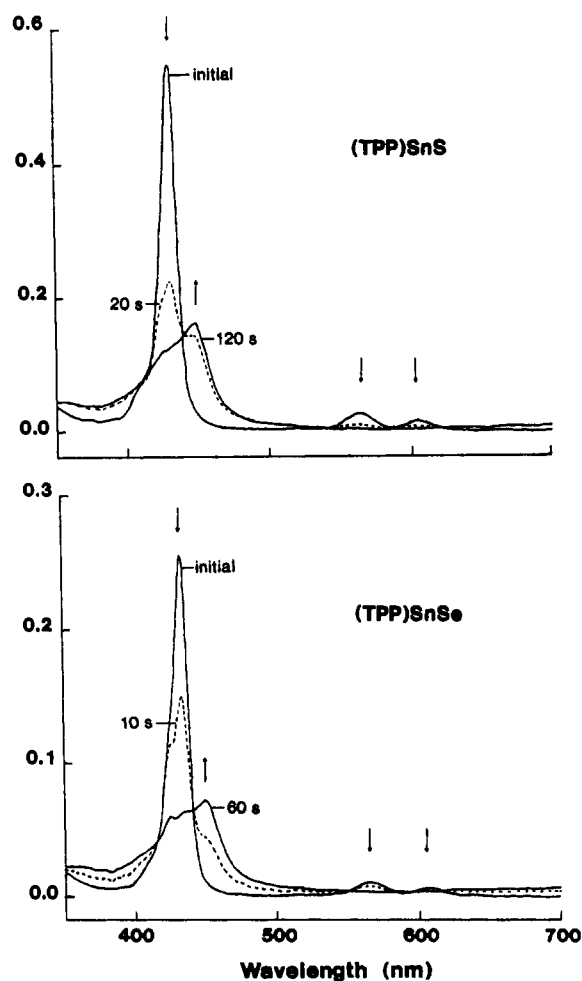


Figure 5. Time-resolved electronic absorption spectra taken during controlled-potential reduction of (TPP)SnS and (TPP)SnSe at -1.10 V in CH_2Cl_2 , 0.1 M TBAP.

during controlled-potential reduction of (TPP)SnS and (TPP)SnSe at -1.10 V. Both reductions are reversible on the thin-layer time scale, and the initial spectrum could be regenerated by applying a controlled potential of 0.00 V after complete electroreduction.

The time-resolved thin-layer spectra in Figure 5 have five isosbestic points, thus implying a simple conversion between the neutral and the singly reduced species. Both final spectra are

characteristic of metalloporphyrin π anion radicals.³⁸ The maximum wavelengths and molar absorptivities are also comparable to values for singly reduced (TmTP)Sn(OH)₂ or (TpTP)-Sn(OH)₂,¹³ thus further suggesting that the first electron addition occurs at the porphyrin π ring system.

The bulk controlled-potential reduction of (P)SnS or (P)SnSe differs from reduction in a thin-layer cell in that the process is no longer reversible and indicates the presence of one or more coupled chemical reactions on the longer time scales required for bulk electrolysis. Bulk controlled-potential reduction of each (P)SnS or (P)SnSe species at -1.10 V also resulted in the consumption of more than two electrons per molecule of metalloporphyrin, consistent with a decomposition of the complex. However the initial transfer of about one electron, as determined from the current-time curves, was accompanied by a change of solution color from green (with a deep red reflectance) to dark green, which is a color often observed for metalloporphyrin π anion radicals. The color continued to change as the electrolysis proceeded and, after the addition of several more electrons, the solution became clear yellow-brown. The overall reduction was irreversible, and the initial UV-visible spectrum of (P)SnS or (P)SnSe could not be regenerated by controlled-potential reoxidation at 0.00 V.

Electrooxidation of (P)SnS and (P)SnSe. The cyclic voltammograms of (P)SnS or (P)SnSe show an irreversible broad oxidation peak located between 0.63 and 0.85 V for a potential scan rate of 0.1 V/s. This peak is ill defined, as illustrated in Figure 5, and has a maximum peak current that is substantially lower than values for the two reversible reductions. The potential of this oxidation peak was not totally reproducible and depended upon the condition of the electrode surface. For example, successive oxidation scans resulted in a shift of E_p toward more positive potentials and at the same time a decreased current was observed. This was especially evident for the sulfur complexes and seemed to result from a poisoning of the electrode surface during oxidation. Similar results were obtained when a glassy-carbon working electrode was used instead of platinum.

The potential difference between the first ring oxidation and the first ring reduction of most metalloporphyrins generally amounts to 2.25 ± 0.15 V³⁵ when the reactions both occur at the porphyrin π ring system. If the same potential separation were obtained for the investigated series of compounds, a ring-centered oxidation of (P)SnS or (P)SnSe would be predicted to occur at $E_{1/2}$ values between 1.26 and 1.40 ± 0.15 V. As seen in Table V, the actual values of E_p range from 0.63 to 0.85 V.

An oxidation of the Sn(IV) central metal cannot occur in (P)SnS or (P)SnSe, and the values of E_p are only consistent with an oxidation at the bound chalcogen axial ligand. Further support for this assignment comes from the fact that (P)Ti(S₂) and (P)Ti(Se₂) both undergo an oxidation of the chalcogen ligand at potentials which range from 0.69 to 1.12 V in the same solvent, supporting electrolyte system.²⁷

The spectral changes which occur during thin-layer controlled-potential oxidation of (TPP)SnS and (TPP)SnSe are shown in Figure 6 and are similar to changes observed during the oxidation of (TpTP)SnS or (TpTP)SnSe. The maximum wavelengths and molar absorptivities of each oxidized complex are summarized in Table V. Oxidized (TpTP)SnSe has a UV-visible spectrum which is identical with that of (TpTP)Sn(ClO₄)₂ (see Table V). In contrast, the spectrum obtained after complete oxidation of (P)SnS at +1.00 V does not result in (TpTP)Sn(ClO₄)₂ but rather gives a spectrum that corresponds to a Sn(IV) porphyrin with some unknown axial ligand. The general spectral pattern is the same before and after oxidation (see Figure 6), but all bands are blue-shifted by about 6 nm after the electrode reaction. This electrooxidation is irreversible, and changes in the spectra were not observed when the applied potential was reset to 0.00 V.

UV-visible spectra obtained after bulk controlled-potential oxidation of (P)SnS or (P)SnSe are in agreement with results

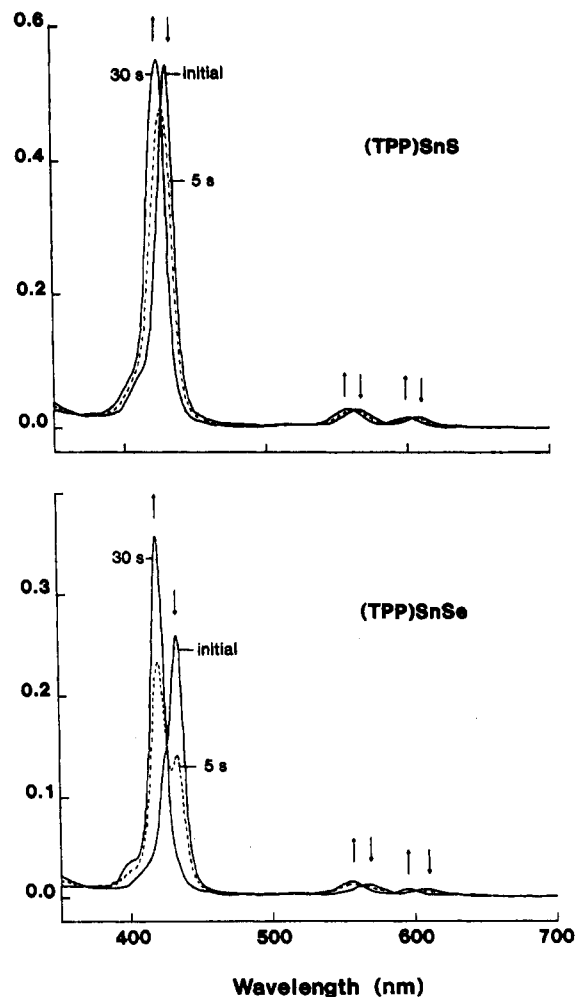


Figure 6. Time-resolved electronic absorption spectra taken during controlled potential oxidation of (TPP)SnS and (TPP)SnSe at +1.00 V in CH₂Cl₂, 0.1 M TBAP.

described above for oxidation in a thin-layer cell. ESR signals were not observed after electrolysis, and no current was passed when the potential was reset to 0.00 V. Controlled-potential coulometry gives a total of 1.0 ± 0.1 electrons abstracted per molecule of (P)SnSe, while a reproducible but low value of 0.25 ± 0.02 electron is obtained for oxidation of the (P)SnS derivatives.

The cyclic voltammograms of solutions containing bulk oxidized (P)SnSe show a well-defined cathodic peak at $E_p = -0.65$ V. This value compares with the -0.65-V reduction potentials reported for selenium powder in THF or DMF³⁹ and in our present study is assigned to reduction of a selenium species generated during electrooxidation of (P)SnSe. A similar reduction peak is not observed after oxidation of (P)SnS, but a yellow material is deposited onto both the walls of the cell and the electrode during electrolysis. This material is identified as sulfur and could be stripped off the electrode by application of a negative potential (-1.60 V) in a fresh solution of CH₂Cl₂, 0.1 M TBAP.

In summary, the overall electrochemical data suggest that (P)SnSe undergoes an initial one-electron oxidation at the selenium axial ligand after which there is a cleavage of the Sn-Se bond, leading to the subsequent formation of (P)Sn(ClO₄)₂. The (P)SnS complexes also appear to be oxidized at the S²⁻ axial ligand, as indicated by the fact that some free sulfur is observed in solution. However, (P)Sn(ClO₄)₂ does not appear to be the porphyrin product in this oxidation. Sulfur is known to be a versatile bridging ligand and, when complexed with many metal or metalloid species, may lead to clusters or polymers.⁴⁰ The coulometric data suggest

(38) Felton, R. H. In *The Porphyrins*; Dolphin, D., Ed.; Academic: New York, 1978; Vol. V, Chapter 3.

(39) Gautheron, B.; Tainturier, G.; Degrand, C. *J. Am. Chem. Soc.* **1985**, *107*, 5579.

that a polymeric form of Sn(IV) may be generated in the oxidation of (P)SnS. Specifically, the reproducible value of 0.25 ± 0.02 electron abstracted is consistent with the formation of a Sn(IV) porphyrin tetramer with the stoichiometry ((P)Sn)₄S₃(ClO₄)₂. This type of species should have wavelength maxima located

between those of the original (P)SnS derivative and (P)Sn(ClO₄)₂, which is exactly what is observed. Unfortunately, all attempts to isolate or further characterize an oxidized form of (P)SnS have so far been unsuccessful.

Acknowledgment. The support of the CNRS and of the National Science Foundation (Grants CHE-8822881 and INT-8413696) is gratefully acknowledged.

(40) Cotton, F. A.; Wilkinson, G. *Advanced Inorganic Chemistry*; Wiley Interscience: New York, 1988; p 491.

Contribution from the Department of Chemistry, University of Houston, Houston, Texas 77204-5641, and Laboratoire de Synthèse et d'Electrosynthèse Organométallique Associé au CNRS (UA 33), Université de Bourgogne, Faculté des Sciences "Gabriel", 6 Boulevard Gabriel, 21100 Dijon, France

Effect of Pyridine Binding and Spin State on Spectroscopic and Electrochemical Properties of Phenyl- and (Perfluorophenyl)iron(III) Porphyrins

K. M. Kadish,^{*1a} A. Tabard,^{1b} W. Lee,^{1a} Y. H. Liu,^{1a} C. Ratti,^{1a,b} and R. Guillard^{*1b}

Received July 31, 1990

The effect of pyridine binding and spin state on the spectroscopic and electrochemical properties of six-coordinate σ -bonded iron(III) porphyrins is reported. The investigated compounds are represented by (P)Fe(R) where P is the dianion of octaethylporphyrin (OEP), tetraphenylporphyrin (TPP), tetra-*m*-tolylporphyrin (TmTP), tetra-*p*-tolylporphyrin (TpTP), or tetrakis(*p*-(trifluoromethyl)phenyl)porphyrin (TpCF₃PP) and R is C₆H₅, C₆F₄H, or C₆F₅. The five- and six-coordinate σ -bonded (P)Fe(C₆H₅) derivatives are low spin in all solvents at room temperature. However, at 100 K in toluene, the ESR spectrum of (TpCF₃PP)-Fe(C₆H₅) is assigned as due to a mixture of the high- and low-spin-state Fe(III) complex. The five-coordinate (P)Fe(C₆F₄H) and (P)Fe(C₆F₅) derivatives are high spin in noncoordinating solvents, but low-spin coordinate iron(III) species are formed in neat pyridine or in pyridine/benzonitrile mixtures. The complexes were investigated by UV-visible, ¹H NMR, and ¹⁹F NMR spectroscopy as well as by electrochemistry and provide the first examples for low-spin (perfluorophenyl)iron(III) porphyrin σ -bonded species. Formation constants for the addition of one pyridine ligand to high-spin (P)Fe(C₆F₄H) and (P)Fe(C₆F₅) were measured in benzonitrile, and these data are compared to related ligand-binding data for low-spin (P)Fe(C₆H₅) derivatives under the same experimental conditions.

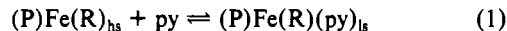
Introduction

A variety of σ -bonded iron(III) porphyrins have been synthesized and spectroscopically or electrochemically characterized²⁻¹⁸ as model compounds in studies involving the metabolic reduction of polyhalogenated derivatives by cytochrome P₄₅₀.¹⁸⁻²⁰

The type of σ -bonded axial ligand and the porphyrin ring basicity will both influence the spin state of the iron(III) atom,^{12-15,17,21,22} and this will be reflected in the spectroscopic or electrochemical properties of a given σ -bonded complex.

σ -Bonded phenyl^{13,14,21} and tolyl¹⁷ porphyrin complexes are low spin at room temperature in benzene or chloroform, while σ -bonded perfluorophenyl (C₆F₅ and C₆F₄H) derivatives of octaethyl- and tetraphenylporphyrins are high spin under the same experimental conditions.^{21,22} Six-coordinate (P)Fe(C₆H₅)(L) derivatives, where P is the dianion of a given porphyrin ring and L is a nitrogenous base, are also low spin,^{15,17} but characterization of spin state in six-coordinate (P)Fe(C₆F₅)(L) or (P)Fe(C₆F₄H)(L) has never been reported.

As will be demonstrated in this paper, the binding of pyridine to high-spin (P)Fe(C₆F₅) or (P)Fe(C₆F₄H) produces a six-coordinate species that is accompanied by a change of spin state according to the following equation:



The resulting six-coordinate complexes are low spin at all temperatures and provide the first examples for low-spin (perfluorophenyl)iron(III) σ -bonded porphyrins.

Previous electrochemical studies have shown that all low-spin (P)Fe(C₆H₅) complexes are relatively stable upon electroreduction,^{14,15,22} while all high-spin (P)Fe(C₆F₅) and (P)Fe(C₆F₄H) derivatives undergo a rapid cleavage of the iron-carbon bond upon the addition of one electron.²² This difference in stability between the phenyl and perfluorophenyl σ -bonded complexes was attributed to the different spin states of the Fe(III) central metals but may also be due to the different axial ligands. This is explored in the present paper, which characterizes electrochemistry of various

- (1) (a) University of Houston. (b) Université de Bourgogne.
- (2) Reed, C. A.; Mashiko, T.; Bentley, S. P.; Kastner, M. E.; Scheidt, W. R.; Spartalian, K.; Lang, G. *J. Am. Chem. Soc.* **1979**, *101*, 2948.
- (3) Lexa, D.; Savéant, J.-M.; Battioni, J.-P.; Lange, M.; Mansuy, D. *Angew. Chem. Int. Ed. Engl.* **1981**, *103*, 6806.
- (4) Clarke, D. A.; Dolphin, D.; Grigg, R.; Johnson, A. W.; Pinnock, H. A. *J. Chem. Soc. C* **1968**, 881.
- (5) Lexa, D.; Mispelter, J.; Savéant, J.-M. *J. Am. Chem. Soc.* **1981**, *103*, 6806.
- (6) Ortiz de Montellano, P. R.; Kunze, K. L.; Augusto, O. *J. Am. Chem. Soc.* **1982**, *104*, 3545.
- (7) Lexa, D.; Savéant, J.-M. *J. Am. Chem. Soc.* **1982**, *104*, 3503.
- (8) Ogoshi, H.; Sugimoto, H.; Yoshida, Z.-I.; Kobayashi, H.; Sakai, H.; Maeda, Y. *J. Organomet. Chem.* **1982**, *234*, 185.
- (9) Mansuy, D.; Battioni, J.-P.; Dupré, D.; Sartori, E. *J. Am. Chem. Soc.* **1982**, *104*, 6159.
- (10) Kunze, K. L.; Ortiz de Montellano, P. R. *J. Am. Chem. Soc.* **1983**, *105*, 1380.
- (11) Battioni, P.; Mahy, J. P.; Gillet, G.; Mansuy, D. *J. Am. Chem. Soc.* **1983**, *105*, 1399.
- (12) Cocolios, P.; Laviron, E.; Guillard, R. *J. Organomet. Chem.* **1982**, *228*, C39.
- (13) Cocolios, P.; Lagrange, G.; Guillard, R. *J. Organomet. Chem.* **1983**, *253*, 65.
- (14) Lançon, D.; Cocolios, P.; Guillard, R.; Kadish, K. M. *J. Am. Chem. Soc.* **1984**, *106*, 4472.
- (15) Lançon, D.; Cocolios, P.; Guillard, R.; Kadish, K. M. *Organometallics* **1984**, *3*, 1164.
- (16) Doppelt, P. *Inorg. Chem.* **1984**, *23*, 4009.
- (17) Balch, A. L.; Renner, M. W. *Inorg. Chem.* **1986**, *25*, 303.
- (18) Balch, A. L.; Renner, M. W. *J. Am. Chem. Soc.* **1986**, *108*, 2603.
- (19) Uehleke, H.; Hellmer, K. H.; Tabarelli-Poplawski, S., *Arch. Pharmacol.* **1973**, *279*, 39.
- (20) (a) Mansuy, D.; Nastainczyk, W.; Ullrich, V. *Arch. Pharmacol.* **1974**, *285*, 315. (b) Wolf, C. R.; Mansuy, D.; Nastainczyk, W.; Deutschmann, G.; Ullrich, V. *Mol. Pharmacol.* **1977**, *13*, 698.

- (21) Tabard, A.; Cocolios, P.; Lagrange, G.; Gerardin, R.; Hubsch, J.; Le-comte, C.; Zarembowitch, J.; Guillard, R. *Inorg. Chem.* **1988**, *27*, 110.
- (22) Guillard, R.; Boisselier-Cocolios, B.; Tabard, A.; Cocolios, P.; Simonet, B.; Kadish, K. M. *Inorg. Chem.* **1985**, *24*, 2509.